Some Topics of Navier-Stokes Solvers

By

H. HONMA*, and N. NISHIKAWA*

(May 1, 1990)

Summary: Process of numerical simulation consists of selection of some items: mathematical model, numerical scheme, level of computer, and post processing. On this point of view recent numerical studies of viscous flows are described especially for the fluid engineering laboratories in the Chiba University. The examples of simulations are Mach reflection on a wedge by kinetic model equation and a cylinder-plate juncture flow by incompressible Navier Stokes equation. Some attempts of graphic monitoring of fluid mechanical calculations are also shown for some combinations of computers with CFD solvers.

1. INTRODUCTION

In this paper the recent numerical studies of viscous flows are described as for the fluid engineering laboratories in the Chiba University.

Today usual descriptions about steps of numerical simulation consist of the following steps:

1. Choice of physical model for a flow and description in mathematical model: e.g. continuum theory or kinetic theory
2. Selection of algorithm together with grid generation technique
3. Choice of computer: workstation, main frame or super computer
4. Development of post processing or graphics monitoring through CFD calculation.

In the fluid engineeing laboratories in Chiba University the investigation recently developed into the items 1, 3, and as for item 2 several schemes have been applied since two decades ago. Thus, the first part of this report is a review of algorithms and its applications by the authors. Circumstances in our laboratories are quite improved as for 3rd and 4th items by Grant in aid for CFD by the ministry of Education from 1987 to 1989. The second part of this report is witten about these items, where processing of graphical output simultaneously with CFD calculation on computers. Some examples of post processing will be also presented.

2. NUMERICAL STUDIES OF COMPRESSIBLE FLOW

Random Choice method was applied for blast waves by Honma et al [1] and inviscid flow around axisymmetric body, while the flow with wall shear flow has not been considered.

2.1 Applied Schemed

FCT algorithm [2] has been applied [3] for inviscid flow taking advantage of shock

*Faculty of Engineering, Chiba University.

capturing capability. The method is recently applied to viscous flow over a wedge [4].

Line Gauss-Seidel scheme was coded [5] to confirm its huge convergence speed. As a result the CFL number as large as 10^{20} was attained for a supersonic flow over a hump [5] and for a three dimensional flow [6]. TVD-Mac Cormack scheme is also applied for an axisymetric flow over a sphere [7] the, a flow over a hamp [8], and a viscous flow around a blunt fin normal to a flat plate [9].

Another topic of compressible flow study in Chiba is the calculation of compressible viscous layer in a rarefied gas flow.

2.2.1 Viscous layer behind shock predicted by kinetic equation

In this calculation the two dimensional unsteady flow is predicted as an extension of the scheme by Morinishi and Oguchi [10]. A BGK type kinetic equation is solved by a MacCormack predictor-corrector scheme. The developed scheme is applied to the problem of nonstationary boundary layer.

Since the nonstationary process occurs mainly within a distance of mean free paths' level behind the leading edge, it is difficult to treat the phenomenon by a continuum approach. Therefore, a kinetic-model approach is used here.

At this study, in order to improve the understanding of Mach reflection of a shock wave at a wedge, the process of formation of Mach reflection is numerically investigated by using a kinetic-model approach. A BGK model equation is described by the reduced distribution functions [10]. The calculations are carried out for a shock Mach number 2.75 and a wedge angle 25° in a monatomic gas. In order to clear the influence of wedge surface conditions on the reflection, the simulations are carried out with and without viscous layer, that is, diffuse and specular reflections of molecules reflection [case I], a nonstationary process from regular to Mach reflection appears at the initial stage of the reflection, while in the case of specular reflection [case II] a quasi-stationary process appears for diffuse reflection exhibit a qualitative agreement with the experimental data [11, 12].

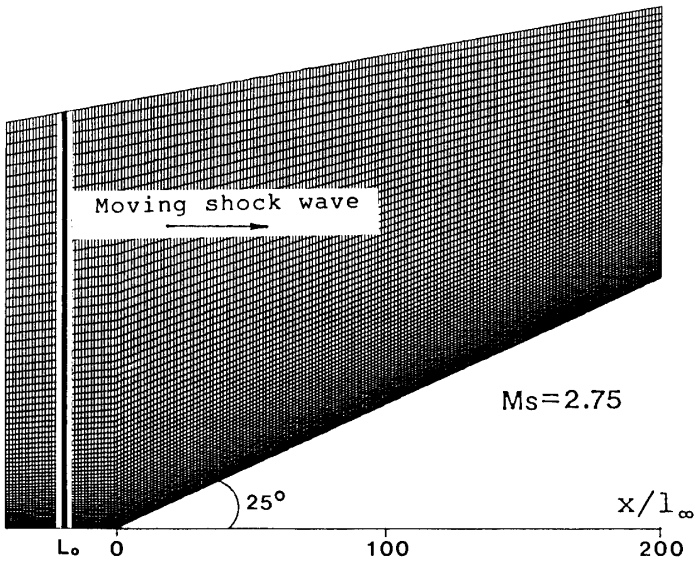

Fig. 1. Flow model and spatial grids.

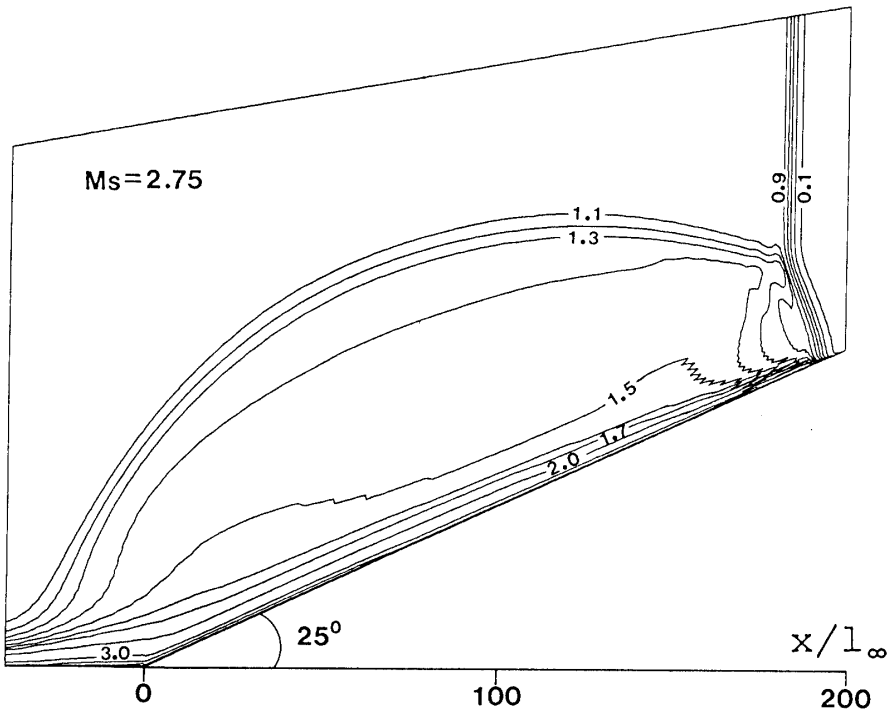

Fig. 2(a). Density contours $(\rho-\rho_1)/(\rho_2-\rho_1)$ in case.

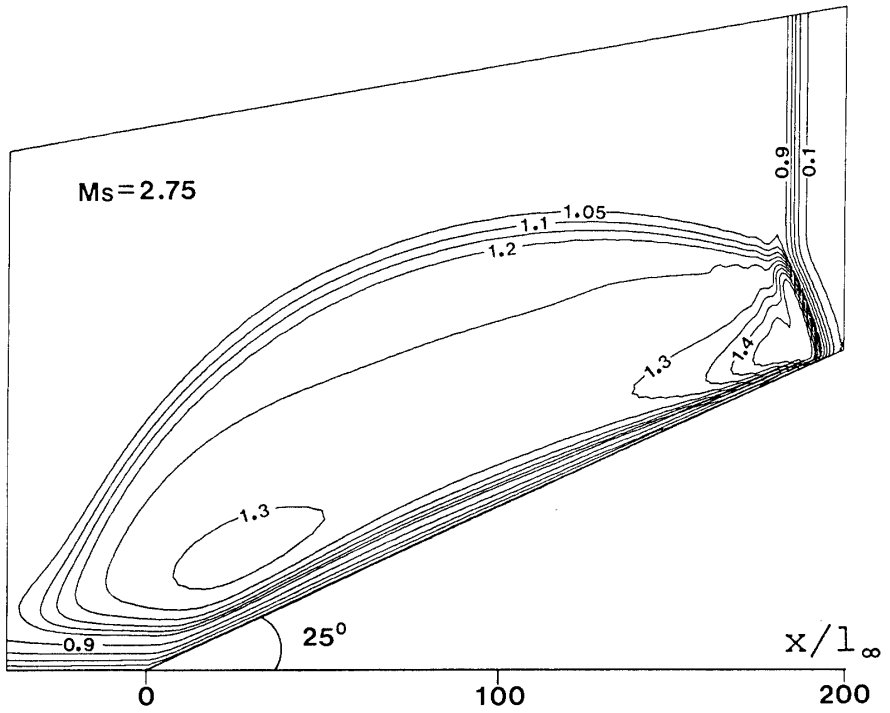

Fig. 2(b). Temperature contours $(T-T_1)/(T_2-T_1)$ in case.

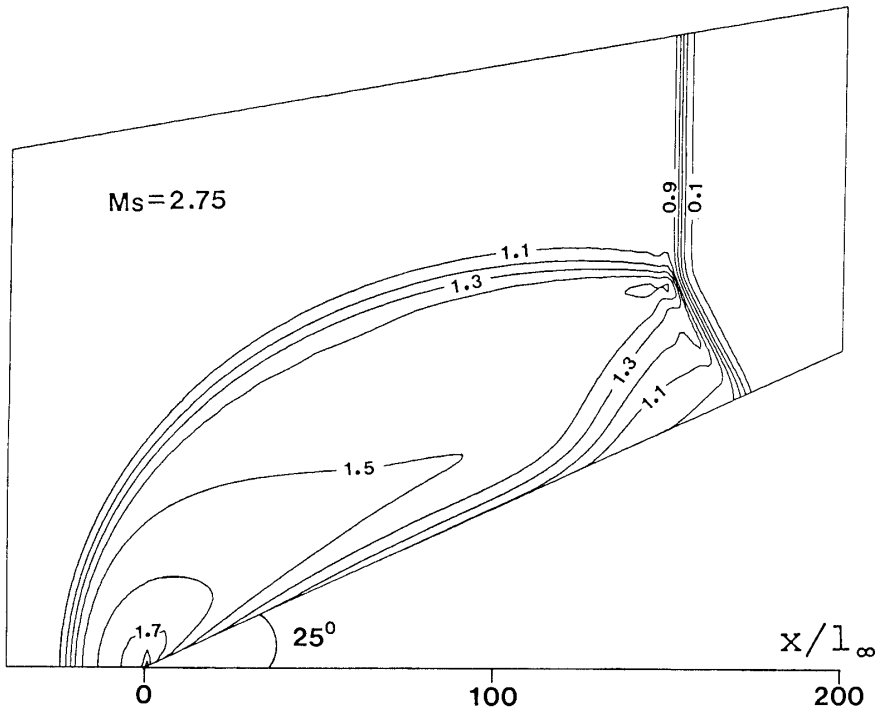

Fig. 3(a). Density contours $(\rho-\rho_1)/(\rho_2-\rho_1)$ in case.

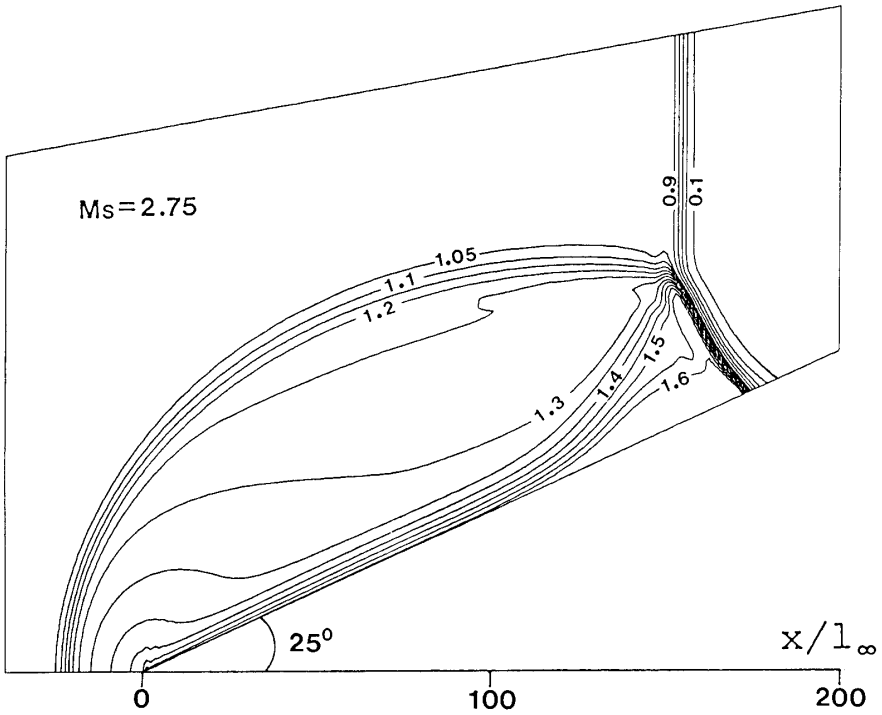

Fig. 3(b). Temperaturs contours $(T-T_1)/(T_2-T_1)$ in case.

The BGK-model equation for two-dimensional flows can be expressed in a non-dimensional form. Here the conception of reduced distribution functions described in Refs. [10] is introduced to reduce the storage and CPU time of the computation.

2.2.2 Numerical Results for BGK model

The flow model and spatial grids are shown in Fig. 1. The shock Mach number is 2.75 and the wedge angle is 25°. This is in the range of SMR (Simple Mach Reflection), according to the shock wave reflection regions indicated by Ben-Dor & Glass [13] for monatomic gases. Calculations are carried out with the Maxwellian molecule model.

As an initial condition, a shock wave with one-dimensional steady structure is given around $x/l_\infty = Lo$ as shown in Fig. 1. The number of grids is 200×70 in the spatial domain, and 20×20 for case I, 24×24 for case II in the velocity domain. The calculations [14] were carried out in the supercomputer Facom VP-200 (ISAS, Japan), the CPU time was 470 minutes for case I and 237 minutes for case II.

Figures 2 (a), (b), show the normalized density, temperature and pressure contours of case I, when the incident shock wave proceeded about 182 l_∞ along the wedge surface behind the leading edge. The normalizations are carried out by using the upstream values (denoted by 1) and downstream values (denoted by 2) of incident shock. The figures clearly exhibit a feature of Mach reflection and also a viscous layer along the wedge surface. The corresponding density, temperature and pressure contours for case II are given in Figs. 3 (a), (b), when the incident shock wave locates about 151 l_∞ behind the leading edge. Though the propagation distance in case II is shorter than in case I, a longer Mach stem is observed in case II. The The reflected shock wave in front of the leading edge is approximately cylindrical and meets the wall perpendicularly, since there is no viscous layer influence in case II.

The distributions of density, temperature, pressure and slip velocity along the wall surface corresponding to Figs. 2 and 3 are given in Figs. 4 and 5, respectively. In the case with viscous layer, there is a large density rise along the gas temperature and velocity along the wall are nearly the same as the values of wall surface except in the vicinity of Mach stem where some jumps can be observed. Whereas in the case without

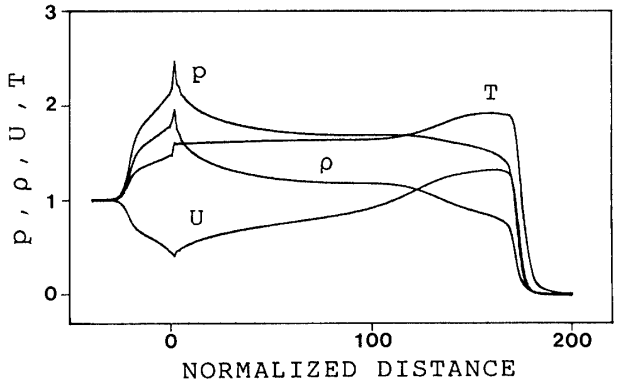

Fig. 4. Distributions of normalized pressure, density, temperature and velocity along the wall surface in case.

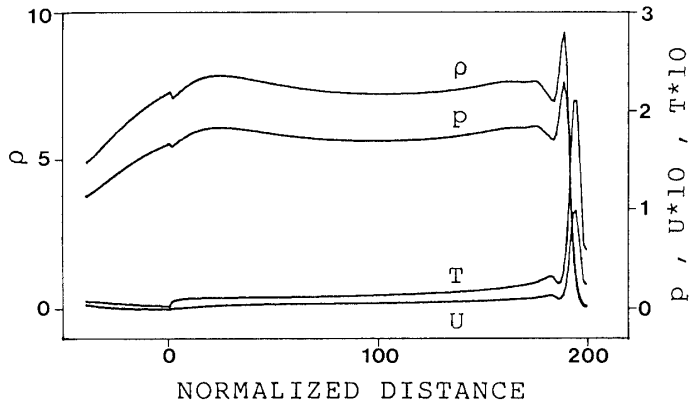

Fig. 5. Distributions of normalized pressure, denslty, temperature and velocity along the wall surface in case.

viscous layer, the density and pressure take their peaks in the leading edge of the wedge. And no acommodation of temperature and velocity to the wall surface be observed.

3. Review of Incompressible Viscous Fiow Solver

The main part of this chapter is the description about finite difference calculations for Navier Stokes equation by the graduate students whose supervisor is Nishikawa. This subject was started after the finite difference calculation of the three dimensional boundary layer by Nishikawa [15].

3.1 Types of Formulations

Among finite difference algorithms for incompressible Navier-Stokes equation, the primitive variable form is widely used and V-ω (velocity-vorticity) form has been challenged. On the other hand applications of ϕ-ψ or ϕ-ω form become less due to difficulty in the assignment of 3-D boundary condition for external flow or complicated boundary conditions.

First, we review the primitive variable formulation briefly. This category contains the following three algorithms. 1. MAC method, 2. Projection Method and, 3. Artificial Compressibility Metohd.

3.2.1 MAC method: This method has been most widely used, especially as SMAC method [16], although viscous term is explicit in contrast to the semiimplicit procedure for velocily-pressure coupled iteration. For Cartesian coordinate this scheme takes the advantage of staggered grid to avoid spati al oscillation of pressure. The implicit treatment of viscous term was presented by Pracht [17].

3.2.2 Projection Method This method, which was proposed independently by Chorin [18] and Temam [19], is two step method where the sencond step can be considered as a projection of provisonal velocity vector onto its subspace with zero divergence. The explicit version was presented by Fortin et al [20] in the group of Temam and is called as Fractional step method. The recent example for projection method is given by Bell & Glaz et al. [21] and the one for fractional step is by Rosenfeld & Kwak [22]. In Japan the projection method was applied for vortex ring by Chen [23]. The Projection method is almost identical to MAC nethod when the staggered MAC mesh is used, as long as boundary conditions are not considered.

3.2.3 Artificial Compressibility Method This method by Chorin [24] is based on the continuity equation with time derivative of pressure, and with divergence term multiplied by artificial 'sonic velocity' c^2. Thus, the method is categorized as a pseudo-unsteady method whose converged solution is that for a steady flow. As far as the formulation concerned this method is identical to the MAC method if the artificial 'sonic velocity' term $\lambda = c^2 \Delta t$ is replaced by the convergence parameter of MAC type method as follows; $\lambda = c^2 \Delta t \rightarrow \lambda = .5 /(1 /\Delta x^2 + 1 /\Delta y^2)$. We should consider whether a solution by this method is for completely incompressible flow.

3.2.4 V–ω Form is also developed by some peoples such as Osswald & Ghia [24] or Labidi &, Ta Phouc [25]. ψ–ω form is successfully applied for twodimensional flow with an ietegro-differential solver by Tokunaga et al [26].

3.3.1 Choice of Differencing Mesh

Staggered Difference form: MAC grid is superior to other differencing for simple geometry or orthogonal grids, since the differencing error $\varepsilon \infty \Delta x$ for mesh increment $\triangle x$. however for general BFC coordinate, as to be descibed later, the coding become lenghty due to cross derivative term, otherwise an un-popular contravariant-physical formulation by Christoffel symbol is introduced.

As far as orthogonal coordinate concerned, non-staggered grid discretization is far less compared to staggerd analogue for multigrid approach [28]. In Japan as for general BFC coordinate the staggered mesh seems to be more popular, than non-staggerred mesh applications [29, 30, 31]. However, for general non-orthogonal boundary fitted grids the non-staggerd discretization is confirmed to be convenient and superior [28]. That is, non-staggerd differencing in general coordinates, is simple for coding, and morever the differencing error is $\varepsilon \infty 2\Delta x$ which is not large if usual staggered differencing is less accurate at skewd grid elesent.

3.3.2 Up-wind Differencing: 3rd Order Artifcial Viscosity

Among relatively new upwind differencing for incompressible Navier-Stokes equation, third order upwind differencing are compared by Kawai & Ando [32] for two dimensional cavity flow. They compared Quick scheme [33], Agarwal scheme [34], and Kawamura scheme [35]. From this comparison it is known that the Quick scheme [33] is best in stability and accuracy, that is, both accuracy and stability fall down in the order Quick > Agarwal scheme > Kawamura scheme for 2-D Cavity. In their test, latter two schmes are stable $Re < 1000$, while Quick scheme keep its stability up to $Re < 5000$.

The relations between the above upwind differencing expressions are clearly discussed by Daiguuji & Yamamoto [36].

3.3.3 Complete Contravariant Physical form

A Contravariant Physical form was generalized and applied to turbulence by Demirdzic, Gosman et al [37] and is recently introduced in a BFC general coordinate by Koshizuka et al [38]. The similar formulation can been seen in the High Reynolds calculation by Watanabe and Oshima [39] and in the 3-D calculation by Takeda [40].

The concepts developed for compressible flow is extended to the incompressible viscous flow as follows.

Incompressible TVD scheme is attempted by some authors, e. g. Gorski [41], Daiguuji et al [30]. Splittinng scheme is applied by Merkle [42] with a scheme almost

similar to artifcial compressiblity method, however the method was extended to unsteady flow.

3.4 Numerical Study of Viscous flow at $Re > 1000$

In this chapter we show a numerical study of three dimensional unsteady internal flow around the cylinder across the rectanglar channel at $Re > 1000$.

The flow behavior at the same configuration around a cylinder across the channel has been clarified with the results for limiting streamlines for $Re < 500$, or the horse-shoe vortex and so on until 1987.

One of the preceding example for this configuration is the calculation by Mitra [43] which predicts slight symptoms of unsteady flow behavior, and where the Reynolds number is not larger than 440 and they used the overlapping coordinate of rectilinear and polar coordinates which needs the 'global' iteration between solutions in each coordinates. However, number of the vortices in front of stgnation point are not predicted accurately by the existing few numerical results; i. e. the number of vortices are different between these results.

For steady external flow around a circular cylinder perpendicular to the flat plate the INS3D code for incompressible N. S. equation has been applied by Kwak et al. [44]. In contrast to the scheme by Mitra [43], the general body fitted coordinate is introduced in their scheme. This code utilizes the Approximate Factorization form and uses a block tridiagonal inversion. Their prediction involves that a secondary flow wraps around the cylinder and a counter rotating pair of vortex filaments. Such AF form is recently applied for the V-ω form Navier stokes equation by Osswald & Ghia [25].

The experimental study for the similar configuration as the above has been reported by Baker [44]. He shows visualization pictures of laminar horse shoe vortex and pressure distributions in the range of Reynolds number frrm 4750 to 10000.

In the present example [46] the finite difference solutions for Navier-Stokes equation are shown for the internal flows, around a cylinder between two flat plates normal the the cylinder.

If we refer the solution procedure the relatively new Navier Stokes solvers, the 3rd order upwind experssion is recommended to be introduced. Thus the present study [46] treated the scheme with 3rd order upwind differencing for convection terms on general curvilinear coordinates. Among the standard style 3-D codes such as SIMPLER, HSMAC, or INS3D, we developed the MAC type solver to the general coordinates.

The solutios are obtained for Re=1800 referred to the cylinder radius with grid distrbution, $52 \times 23 \times 25$, respectively along cylinder azimuthal direction, along the cylinder axis, and lateral direction. The down-stream end of channel is located at 10 D from the cylinder center (D: cylinder diameter) where the extrapolation condition applied and the inlet condition is held as fully developed flow: two dimensional Poiseille profile along vertical direction.

The two dimensional grid generated by elliptic p. d. e is stacked up vertically to the bottom to form a three-dimensional grid. A concentrated mesh distribution are used near the solid surfaces such as the cylinder surface and the channel walls. The Navier Stokes equation is integrated by explicit Euler Method and Poisson equation of pressure is solved by S. O. R scheme. The calculations were carried out in the supercomputer

Facom VP-400, and the CPU time was 110 minutes for 2800 time steps up to t/UD= 8.79.

The qualitative behavior of the flow field predicted is analogous to the results by Kwak et al [44] or Mitra et al [43] as for the structure near the symmetry horizontal plane where two dimensionality prevails. However, the details for the spiral vortex behind the cylinder or for the twin vortex was predicted by us not by Mitra et al [43].

Comparison with the visualization study [47] implies good agreement as 20% deviation of the location of front saddle point.

In Figs. 6 the instantaneous streamlines on the bottom plate of the channel normal to the cylinder are shown and the twin vortices can be observed.

In Fig. 7 the instantaneous streamlines around the cylinder is visualized. The contours of vorticity is shown in Fig. 8 where the contours at each cross-section is traced to make the perspective view from the same direction as in Fig. 7.

Fig. 9 shows pressure coefficient: Cp distribution along cylinder surface at some levels from the bottom of channel. The deviation from 2-D flow behavior is large near the bottom.

3.4. Some future subjects for Incompressible Viscous Flow

Staggerd differencing on general coordinates requires several interporation process for estimating unknowns at midpoint of grid links, because the system of equations involve cross-derivatives of primitive variables along all grid links. While, non-staggered scheme users encountered with the oscillation or wiggle of spatial distribution of pressure, if they use HSMAC type solver. If we choose staggered mesh, it is necessary

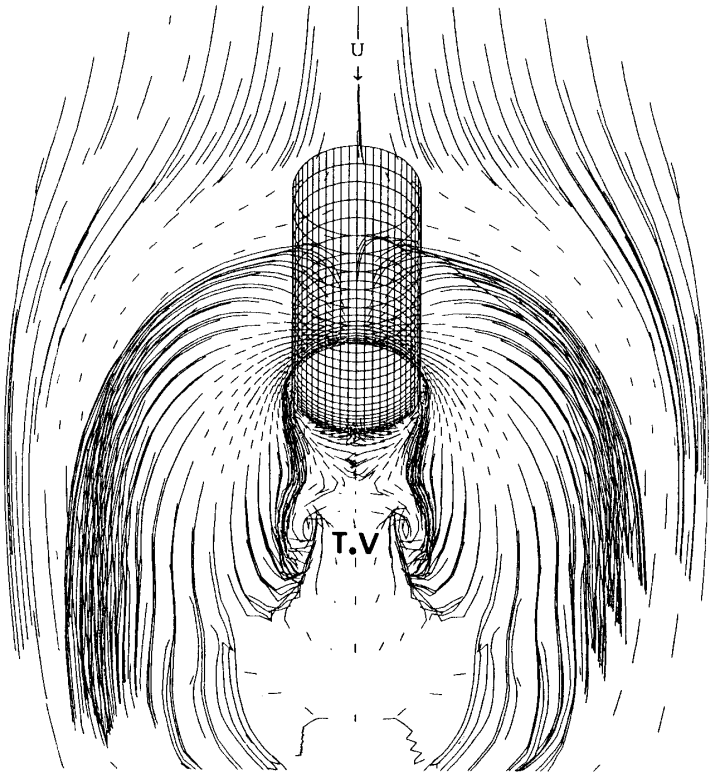

Fig. 6. Surface streamline on the flat vlate: Re=1800, t=8.79.

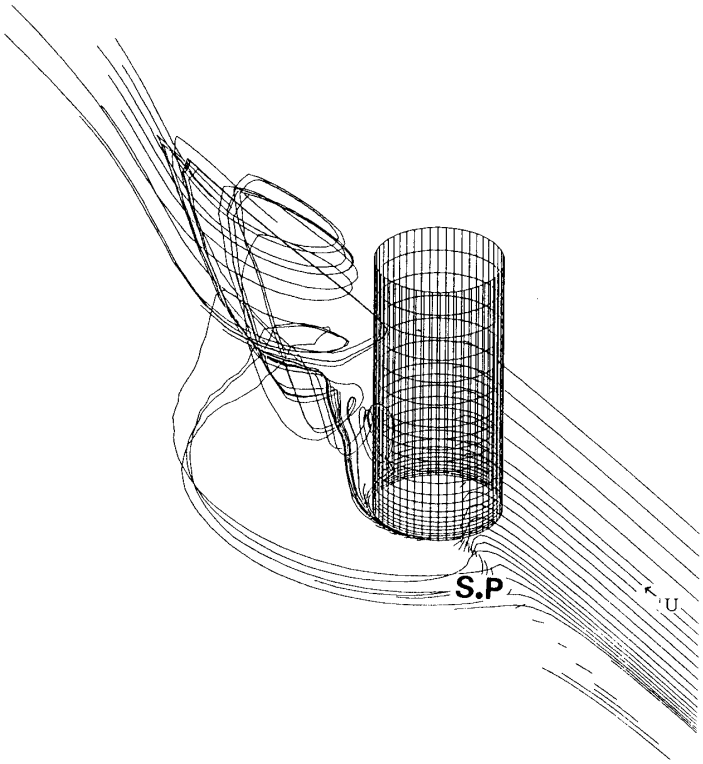

Fig. 7. 3-D Instantaneous streamlines t=2.51.
S.P. SAPPLE POINT

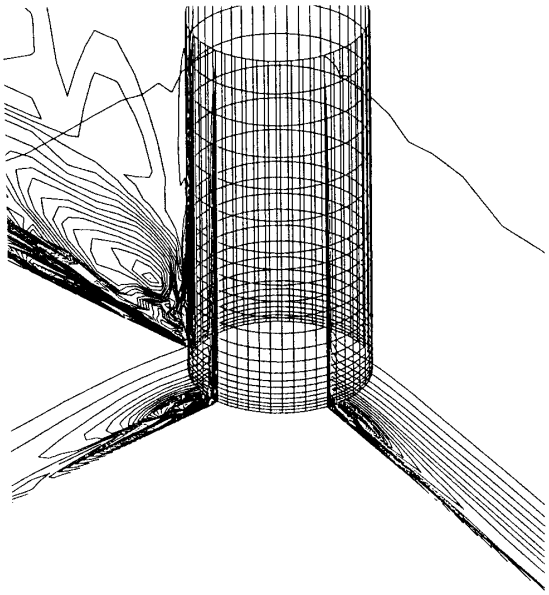

Fig. 8. Vorticity contour.

to apply contravariant physical formulation [37] to avoid sbove mentioned situation and to simplify the code.

Although disadvantage appears in the large calculation time for Christoffel symbols, fully contravariant-physical formuration is promising and resistible to inclination or skewness of grid element.

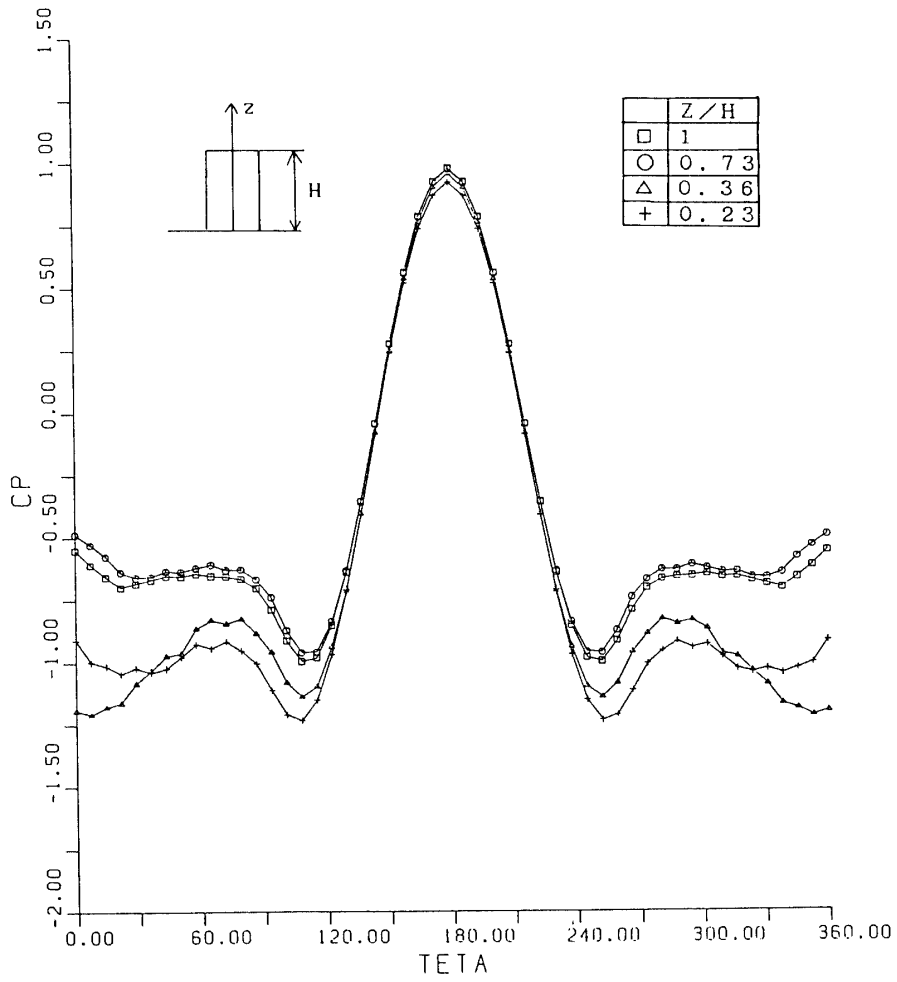

Fig. 9. Cp Distribution along cylinder surface.

The reduction of total amount of operation in the pressure relaxation, which consumes 80% of CPU time, is one of the subjects. For this aim, the method such as Zebra scheme, Multi Grid method has to be applied to accelerate the relaxation. Instead of point relaxation the method, some techniques have been proposed such that assigning velocities as unknowns on the links of a single grid element [48] or on those of multiple grids as in group explicit method [49]. By treating all velocities as unknowns on a grid line, Vanka proposed the box-line scheme [50] with multi grid method.

4. Monitoring of CFD jobs on Mainframes and Graphic Computer [51]

In this chapter graphic monitoring examples are shown for several combinations of numerical schemes with computers such as mainframe, workstation and personal computer. The examples on a graphic computer are also discussed. The computers except mainframe [HITAC-280-IAP] belong to the laboratories of Honma or Nishikawa.

For constructing environment for numerical computation, wide variations of graphical monitoring of CFD jobs are required. But such moitoring seems to be not used

widely. It is usual that once a CFD job has started the detail of temporal profiles cannot be examined with monitoring on character display and the judgement to abort the job is delayed. On the other hand if one can monitor the temporary solutions during calculation with graphical image, the environments of debugging and CPU-load are improved dramatically.

Here the most important example of the attempts may be graphical monitoring on mainframe under restricted data-exchange rate and standard computer power; that is, the restrictions of Japan-standard bps rate as low as 9600 bits/sec and insufficient power of the HITAC-280-IAP with 20 MFLOPS peak performance.

Table 1 contains the educational examples of monitoring on 16 bit computer, on which a Panel Method was applied to the aerofoil, and academic test cases examined here are SMAC scheme for 2-D Navier Stokes equations [48], an Explicit-TVD scheme for 2-D compressible flows through venturi or around sphere, and HSMAC code [31] for the flow around a cylider in channel for incompressible three dimensional Navier-Stokes equation.

The results for single venturi (planar flow) show good agreement with experisental pressure [51]. The pressure and velocity vectors are shown for Re=20000 in Figs. 10, 11 for two values of dimensionless time, which are obtained by HSMAC code. The separation just behind the throat and the four or five attatched vortical regions are predicted.

In Table 2 the timing chart of graphic monitoring on 9600 bps terminal under 20 MFLOPS mainframe is thown for the graphic monitoring of single Cp curve: pressure distribution. The graphic package for the mainfram HITAC-280 is GPSL. At arbitrary timing the monitoring TSS job is submitted to display the data which shared by CFD job at any timestep of fluid mechanical calculation. If the image on the display suggests any fatal aspects at past or future of time marching, the CFD job should be aborted. The

Table 1. Elapse Time for CFD and Monitoring

OS/bit Computer	MS-Dos 16 bit MS (PC) FORTRAN	LATTICE-C	UNIX C 32 bit	UNIX FOR-TRAN MINISUPER	VOS-3 HITAC M-280H-IAP
NUMERICAL SCHEME FLOW CONFIGU & ELAPSE TIME for CFD sec/Grid	Panel method Wing 40 Panel (NACA0015) 90~ 210 SE	Panel method Wing	SMAC A prob. 0.015S	SMAC A prob. 0.003S TVD B prob. 0.0015S	SOLA HSMAC A prob. 3-D CYLINDER-PLATE JUNCTURE TVD B prob. 0.0004S
Monitoring sec Example	2sec	2sec		Dore 1s Fig. 12	EKAKU *GPSL MOVIE-BYU 16s 52s 20s
BPS				(128×2 MBS)	1.2KBS 9.6KBS 128KBS

A prob. Splash of Droplet : Grid 40×30
B prob. Inviscid Compressible VENTURI : Grid 50×20
* E time for diagonal line

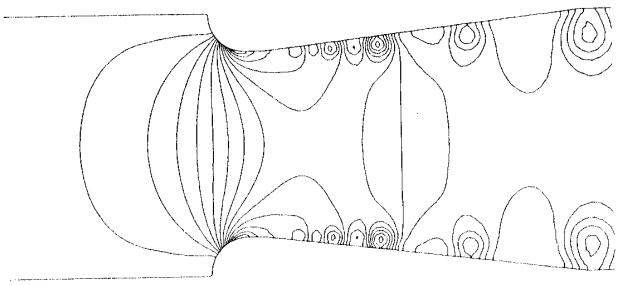

Fig. 10. Pressure contour in venturi by HSMAC scheme: Re = 20000 dimensionles time T = tU/D = 2.0.

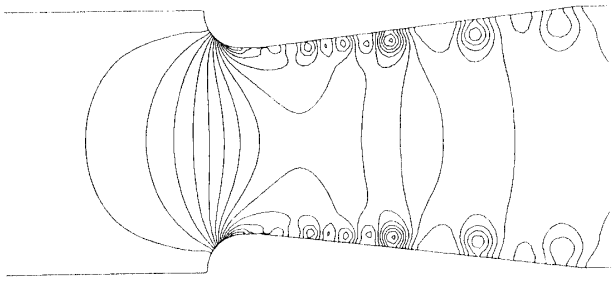

Fig. 11. Pressure contour in venturi by HSMAC scheme: T = 2.5

Table 2. Monitoring of 2-D Euler Solution: Cp curve through 400 dots.

CFD Job	→ 20 TIMESTEP	→ W. DATA	→ 20 TIMESTEP	→	
	WRITE DATA	→ READ &	READ &	↗	
G Job		DISPLAY 52SEC	DISPLAY 52SEC		

G Job = Monitor TSS CFD Job 200SEC/20 TIMESTEP
* If ill symptom appear in monitor
CFD job should be aborted.

Table 3 CG Monitoring of 3-D N. S. Solver

CFD Job	COMPILE, LINK → 3 TIME STEP	→ W. DATA	→ 3 TIME STEP	→ W. DATA	→ ···
	(165SEC)	↓	(165SEC)	↓	
GRAPHIC Job		READ & DISPLAY		READ & DISPLAY	
		(120SEC)		(120SEC)	

interval of the data sharing and monitoring is designed from the comparison of elapse time for the fluid mechanical calculation per time step and that for displaying the graphics. If we observe the elapse time for MOVIE-BYU listed in lower-right corner of Table. 1, it is shown that a full color 3-D image can be also displayed by TSS job co-running with CFD job as shown in the timing chart of Table 3. This example is available when the terminal is connected to CPU via channel at high bps as 128 Kbytes /s. Thus, The example of 3-D HSMAC code is shown in a three dimensional image.

On a graphic computer TITAN I the splashing scene as in Fig. 12 by SMAC

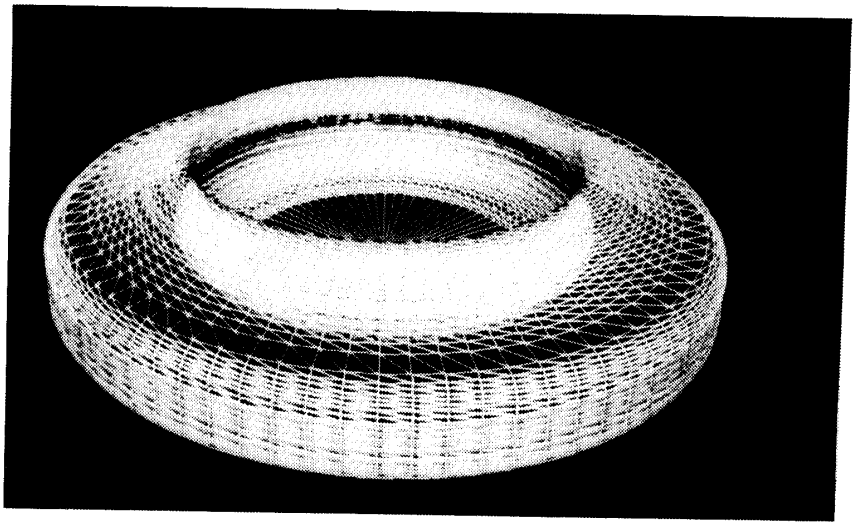

Fig. 12. Surface shape of free surface: Wire frame on TITAN.

calculation can be displayed nearly in real time mode. That is, the shape of free surface can be displayed on each 5 seconds or each 10 time steps. When we use TITAN for the graphic, the graphic tool Dore is not easy to handle because the user need to remember many unfamiliar sub-commandss. Although, cost performance is not so bad at effectively 3 MFLOPS for TVD codes, the vectizer, with which square root operation cannot be vectized, should be improved.

5. Conclusion

In first part of this report the recent CFD studies in Chiba University is introduced and the incompressible Navier-Stokes solvers are extensively reviewed as for typical finite different schemes. In Chiba University the CFD studies are expected to be develped, although the some of obtained results by now are carried out at supercomputer outside the university.

In second part of this report the efficiencies in the graphical monitoring of temporary distributions of flow variables are examined for CFD jobs on wide levels of computers. On the graphic workstation TIATN the fast monitoring of any figures is easy together with fluid dynamics calculation. However, on a main-frame conventional graphics package at 9600 bps are applied, such that executing TSS job to display 3-D color figures or single curve or contour plots with reading the data from running CFD job.

References

[1] Honma, H, Glass, I. I. Proc. Roy. Soc. London, A391, 55–83 (1984)
[2] Boris, J. B., NRL Memorandum Report 3237 (1976)
[3] Honma, H. Wada, K. Inomata, ISAS Report. SP No2, 3–14 (1984)
[4] Honma, H., Maekawa, H., Proc. 3rd Symp. CFD, 147–150 (1989, in Japanese)
[5] Suzuki, A., N. Nishikawa, Proc. 5th Symp. Aircraft Computational Aerodynamics, 233–240, MAL–SP–7 (1988, in Japanese)

[6] Hajima, Y., Master of Engng. Thesis, Chiba University (1990. 3)
[7] Suzuki, T. Master of Engng. Thesis, Chiba University (1988. 3)
[8] Akune, O., Nishikawa. N., Proc. 2nd Symp. CFD, 487–490 (1988, in Japanese)
[9] Suzuki, T., Y. Hajima, N. Nishikawa, Proc 21st Conf. Fluid Mechanics 2-5 (1989, in Japanese)
[10] Morinishi, K. and Oguchi, H., Rarefied Gas Dynamics, Vol. I, 149, ed. H. Oguchi (1984). And doctor thesis of K. Morinishi, Univ. Tokyo.
[11] Walenta, Z. A., Arch. Mech., 35, 2, pp. 187–196, Warszawa (1983).
[12] Walenta, Z. A., Shock Waves and Shock Tubes, 535, ed. H. Groning (1987).
[13] Ben-Dor, G., Glass, I. I., Journal of Fluid Mechanics, Vol. 96, Part 4, 735–756 (1980).
[14] Xu, D. Q., Honma, H. Abe, T., International Symposium on Computational Fluid Dynamics, Nagoya (1989). To be published.
[15] Nishikawa, N., Trans. Japan Soc. Aeron. and Space Science, Vol. 28, 27–43 (1985)
[16] Amsden, A. A. & Harlow, F. H., Los Alamos Res. Labo. La–4370 (1970)
[17] Pracht, W. E. J Comput. Phys., Vol. 7, 46–60 (1971)
[18] Chorin, A. J. Math. Comput., Vol 22. 745–762 (1968)
[19] Temam, R. Archiv. Ration. Mech. Anal. 32. 377–385 (1969)
[20] Fortin, M., Peyret. R., Temam. R Lecture Notes in Physics, No. 8, 337–342 (1971) [See also J. Mec. 10, 357–390 (1971)]
[20] Bell, J. B., Glaz, H. M. Solomon, J. M. & Szymczack, W. G. Lecture Notes in Physics, No. 323, 142 –146 (1989) or [AIAA Paper 87–1176]
[22] Rosenfeld, M. Kwak, D Lecture in Physics, 0. 323, 506–511 (1989)
[23] Chen, H. L. ISAS (Japan) Report SP–5, (1987)
[24] Chorin. A. J. Comput. Phys., Vol. 2 12–26 (1967)
[25] Osswald, G. A., Ghia, K. N. and Ghia, U. Lecture Notes in Physics, No. 323, 454–4461 (1989)
[26] Labidi, Ta Phouc L., Lecture Notes in Physics, No. 323, 354–359 (1989)
[27] Tokunaga, H., Satofuka, N., Yoshikawa, T. AIAA Paper 87–1175 (1987)
[28] Linden, J. et al, Proc. 11th ICNMFD [Invited lecture] (Springer) p57
[29] Shirayama, S. Doctral Dissertation, Univ. Tokyo, (1987. 3)
[30] Daiguuji, H., Itoh, K., Ozaki. T, Proc. 1st Symp. CFD, 9–12 (1987).
[31] Nishikawa, N., Akiyama, S., & Akune, O. Lecture Notes in Physics, No. 323, 439–443 (1989)
[32] Kawai, M. & Ando, Y. J. Jap. Mech. Eng Vol. 52 p2067 (1986)
[33] Leonard, B. P, "Computational Methods in Fluids", Pentech Press 159–195 (1980)
[34] Agarwal, R. K. AIAA-Paper 81–0112 (1981)
[35] Kawamura, N. Kuwahara, K. AIAA Paper 840340 (1984)
[36] Daiguuji, H., Yamamoto, S., Proc. 3rd Mymp. Aircraft Computational Aerodynamics, 267–276, NAL –SP–7 (1986, in Japanese) o.
[37] Demirdzic, I. Gossman. A. D., Issa, R. I. & Peric, M. Computer & Fluids Vol. 15, 251–273 (1987)
[38] Koshizuka et al, Proc Intn. Symp. CFD-Nagoya, 1192–1197 (1989)
[39] Watanabe, Y. Oshima, Y. Proc Intn. Symp. CFD-Nagoya, 659–664 (1989)
[40] Takeda, H., Hsu, C. Z. Proc. 3rd Symp. CFD, 499–502 (1989)
[41] Gorski, J. J. Lecture Notes in Physics, No. 323, 376–282 (1986)
[42] Merkle, C. L. & Athavale M. M., Lecture Notes in Physics, No. 323, 403–407 (1989)
[43] Mitra, N., Kiehm, P., Fiebig, M., Proc. 10th-ICNMFD-Springer 481–487 (1986)
[44] Kwak, D. et al. AqIAA J. Vol. 24 p390–396 (1986)
[45] Baker, C. J. J. Fluid Mech 95, p347–367 (1979)
[46] Akune, O., Nishikawa. N., Proc. 3rd Symp. CFD, 479–482 (1989)
[47] Nishikawa, N., SuzukiT., Trans. Jpn. Aeron. Sp. Sci. Vol. 31, 61–66 (1988)
[48] Nishikawa, N., Suzuki, T., Akiyama, S. Lecture Notes in Physics No. 264, 10th Intn. Conf. Numerical Methods in Fluid Dynamics, 499–504 (1986)
[49] Murata, S., Satofuka. N.,. Proc. 3rd Symp. CFD, 483–486 (1989)
[50] Vanka, S. P. J. Compu. Physics, 65, 138–156 (1986).
[51] Akune, O., Nishikawa. N., Proc. 2nd Symp. CFD, 487–490 (1988)